Biophysical Chemistry 150 (2010) 23–28

Contents lists available at ScienceDirect

Biophysical Chemistry

journal homepage: http://www.elsevier.com/locate/biophyschem

Signal relay from sensory rhodopsin I to the cognate transducer HtrI: Assessing the critical change in hydrogen-bonding between Tyr-210 and Asn-53

Ionela Radu [a,b], Ivan L. Budyak [c], Torben Hoomann [b], Young Jun Kim [d], Martin Engelhard [d], Jörg Labahn [c], Georg Büldt [c], Joachim Heberle [a,b,c,*], Ramona Schlesinger [c,*]

[a] Freie Universität Berlin, Department of Physics, Exp. Molecular Biophysics, Arnimallee 14, 14195 Berlin, Germany
[b] Universität Bielefeld, Department of Chemistry, Biophysical Chemistry (PC III), 33615 Bielefeld, Germany
[c] Forschungszentrum Jülich, Institute of Structural Biology and Biophysics (ISB-2), 52425 Jülich, Germany
[d] Max Planck Institute of Molecular Physiology, Otto-Hahn-Str. 11, 44227 Dortmund, Germany

ARTICLE INFO

Article history:
Received 29 January 2010
Received in revised form 25 February 2010
Accepted 26 February 2010
Available online 2 March 2010

Keywords:
Phototaxis
Signalling state
Signal transduction
FT-IR difference spectroscopy
Isothermal
Titration calorimetry
Bacteriorhodopsin

ABSTRACT

Sensory rhodopsin I (SRI) from *Halobacterium salinarum* mediates both positive and negative phototaxis in a light-dependent manner. SRI photoactivation elicits extensive structural changes which are transmitted to the cognate transducer (HtrI). The atomic structure of the SRI–HtrI complex has not been solved yet and, therefore, details on the interaction which define the binding site between receptor and transducer are missing. The related complex SRII–HtrII from *Natronobacterium pharaonis* exhibits a hydrogen bond between the receptor Y199 and transducer N54. This bond has been suggested to mediate signal relay in the SRII–HtrII system. Our previous results on the SRI–HtrI complex indicated that HtrI N53 forms a hydrogen bond at the cytoplasm-proximity of the membrane. Here, based on kinetic and spectroscopic data, we demonstrate that Y210 of SRI is functionally significant for the signal relay in the SRI–HtrI complex. Each of the tyrosine residues Y197, Y208, Y210 and Y213 were conservatively exchanged for phenylalanine but only the Y210F mutation led to the disappearance of the infrared band of the terminal amide C=O of N53. From this FT-IR spectroscopic result, we conclude that Y210 of SRI and N53 of HtrI interact via a hydrogen bond which is crucial for the signal transfer from the light receptor to the transducer.

1. Introduction

Sensory rhodopsin I (SRI) and sensory rhodopsin II (SRII) from the haloarchaeon *Halobacterium salinarum* mediate attractant and/or repellent phototaxis responses in the cell [1]. Sensory rhodopsins are seven-transmembrane helical retinylidene proteins exhibiting high homology to the ion pumps bacteriorhodopsin (BR) and halorhodopsin (HR). They physically couple with their cognate transducer proteins (HtrI and HtrII) to form tight 2:2 complexes in the membrane [2–4]. The transducers consist of two transmembrane helices (TM1 and TM2) with a long rod-like cytoplasmic domain that controls the flagellar motor via a two-component signalling pathway [5]. Transducer chimera studies indicated that the TMs of the transducers comprise the binding domain to the cognate receptors [6].

Orange light excitation of SRI_{587} triggers a cyclic photochemical reaction which is strongly pH-dependent in the absence of transducer [7]. The formation of the long-lived M-like S_{373} leads to a photoattractant response via helix-helix interactions of the receptor with HtrI. S_{373} is photoactive and its excitation with near-UV light elicits repellent responses in the cell. HtrI-free SRI functions as a light-driven proton pump, yet, with a lower efficiency than BR. The association with HtrI inhibits proton pumping by SRI and renders the photoreaction pH-insensitive [8]. There is a wealth of information regarding the chemical and structural changes in the SRI–HtrI complex but the molecular mechanism of the signal relay from the receptor to transducer still remains elusive.

The crystal structure of the SRII–HtrII complex from *Natronobacterium pharaonis* revealed that Y199 on helix G bridges N74 on TM2 via a hydrogen bonding which is maintained in the signalling state [3,9].

In the present work, we used isothermal titration calorimetry, kinetic UV–Vis and static FT-IR spectroscopy to search for evidence about the existence of tyrosine–asparagine interactions in the SRI–HtrI complex. This investigation is based on our previous infrared results which highlighted N53 on TM2 as a hydrogen-bonded residue important for receptor-transducer interaction [10]. In this study, we focused on the four tyrosine residues (Y197, Y208, Y210 and Y213) on helix G of SRI to check for their ability to associate with N53 (Fig. 1). Thus, each of the single tyrosine residues was conservatively replaced

* Corresponding authors. Heberle is to be contacted at Freie Universität Berlin, Department of Physics, Exp. Molecular Biophysics, Arnimallee 14, 14195 Berlin. Schlesinger, Forschungszentrum Jülich, Institute of Structural Biology and Biophysics (ISB-2), 52425 Jülich, Germany.
E-mail addresses: joachim.heberle@fu-berlin.de (J. Heberle), r.schlesinger@fz-juelich.de (R. Schlesinger).

0301-4622/$ – see front matter © 2010 Elsevier B.V. All rights reserved.
doi:10.1016/j.bpc.2010.02.017

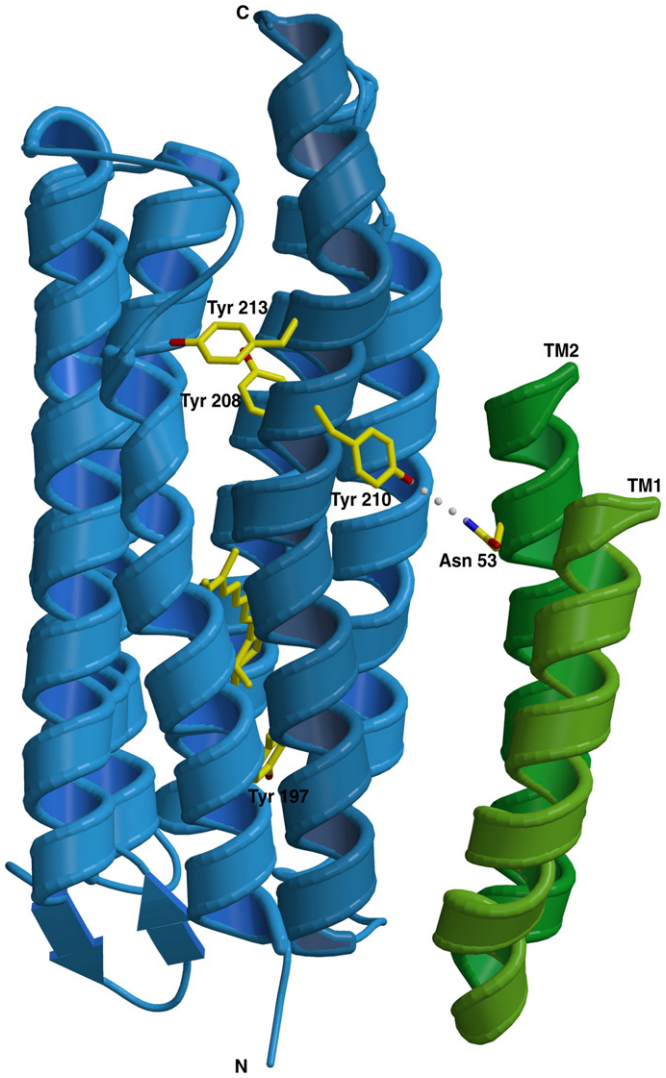

Fig. 1. Model of the SRI–HtrI complex based on the crystal structure of SRII–HtrII complex from *N. pharaonis* (Protein Data Bank access code 1H2S [3]). The transmembrane helices are depicted as ribbons (SRI in blue and HtrI in green). The model highlights the tyrosine and asparagine residues that are the subject of the present work. SRI was modelled by Swiss-Modeller based on the structure of SRII and HtrI from *H. salinarum* was aligned to HtrII from *N. pharaonis* according to the following sequences (α-helical structures are underlined):
HtrII-Np 10-LPSRVRHSYTGKMGALVFIFVGALTVLFGAIAYGEVTAAAAGDAAAVQEAAVSAILGLIILLGINLGLVAATL-82.
HtrI-Hs 2-TIAWARRRYGVKLGLGYIATAGLLVGVGVTTNDV----------PSTIVAGIAGLLTLGSINAAETV-58.
The resulting model of the complex was energy-minimized in CNS.

by phenylalanine. We found by FT-IR difference spectroscopy that the phenolic group of Y210 is the hydrogen-bonding donor to amide carbonyl oxygen of the side chain of N53 of HtrI. This characteristic hydrogen bond is lost in the S_{373} state.

2. Materials and methods

2.1. Plasmids and strains

For DNA manipulations, *E. coli* strain Top10 (Invitrogen) and for gene expression Epicurian Coli® BL21-CodonPlus™(DE3)-RP (Stratagene) were used. The construction of the recombinant *sopI* gene and the resulting primary structure of SRI have been described in [10]. To replace Y197, Y208, Y210 and Y213 by F, the corresponding triplets were substituted by oligonucleotide-directed mutagenesis to TTC or TTT. Upstream of the *sopI* gene, an *Nde*I site was introduced and downstream after the coding region for a 10xHis tag and the stop codon a *HindIII* site was added. The resulting fragment was cloned into the corresponding sites of the pET27 b expression vector (Novagen). Construction of the fusion protein SRI–$HtrI_{1-147}$ (residues 1–147 of the native HtrI) and SRI–$HtrI_{1-52}$ with a C-terminal 6xHis-tag have been described in [10]. The exchange of Tyr to Phe in SRI-$HtrI_{1-147}$ has been done in analogy to the mutagenesis procedure of the receptor which is described above. The fragments were incorporated into pET27 b.

2.2. Expression, purification and reconstitution into polar lipids

For the production of mutated SRI and its fusions with $HtrI_{1-147}$, *E. coli* BL21(DE3) RP cells were transformed with the pET27 b constructs and propagated at 37 °C in double yeast tryptone medium supplemented with 50 mg/l kanamycin. At an OD_{600} of 0.6–0.8, expression was induced by adding 0.2 mM isopropyl-β-D-thiogalactopyranoside. Simultaneously, 12 μM of all-*trans* retinal (Sigma) were added to supply the synthesized opsin with all-*trans* retinal. The cells were pelleted 3–4 h post-induction by centrifugation. A high expression level was indicated by the intense blue color of the harvested cells. Purification was done essentially as described [10,11]. Pelleted cells were resuspended in 500 mM NaCl, 50 mM MES (2-(N-morpholino)ethanesulfonic acid) pH 6.0, 2 mM EDTA (ethylenediaminetetraacetic acid) (~1:10 *w*/*v*) and passed three times through an EmulsiFlex-C3 (Avestin). The insoluble fraction

which contains the membrane proteins was harvested by centrifugation (130,000 g, 30 min, 4 °C) and solubilized overnight at 4 °C in 4 M NaCl, 50 mM MES pH 6.0, 2% (*w*/*v*) DDM (n-dodecyl-β-maltoside; Glycon). After a second centrifugation step, the soluble extract was applied twice to a chromatography column with Ni-NTA agarose (Qiagen) equilibrated with 4 M NaCl, 50 mM MES pH 6.0, 0.05% (*w*/*v*) DDM. Four washing steps have been carried out: (i) with the buffer used for equilibration until the flow through is released as a colorless clear liquid, (ii) with ~10 bed volumes of the same buffer plus 10 mM imidazole, (iii) with ~10 bed volumes of the buffer with 25 mM imidazole, and finally (iv) ~10 bed volumes in the absence of imidazole. Elution was done with the buffer at pH 4.5 and the eluate was immediately diluted with buffer at a final pH in the range of 5.5–6.0. The ratio between the absorption of the protein aromatic residues at 280 nm and the absorbance of the bound chromophore at 587 nm was in the range of 1.6–1.8, which are typical values for pure SRI samples [11,12]. The A_{280}/A_{587} ratio for the fusion proteins was in the range of 2.0–2.2. All investigated proteins were reconstituted into polar lipids from *H. salinarum* as described previously [10,13].

2.3. Isothermal titration calorimetry (ITC)

ITC measurements were carried out using an automated Omega titration calorimeter (MicroCal, Northampon) [14]. The samples were gently degassed before being added to the calorimeter cell. Typically, ~300 μM SRI solubilised in 0.05% DDM, was injected in 12 μl increments into the reaction cell (cell volume 1.5 ml) containing detergent–solubilized HtrI at a concentration of 20 μM until complete saturation. A 290 μl injection syringe with 290 rpm stirring was used to give a series of 12 μl injections at 3 min intervals. Titrations were performed at 20 °C or 25 °C. Control experiments for heats of mixing and dilution were performed under identical conditions and used for data correction in subsequent analysis. Data evaluation was done in terms of a simple binding model, using the ORIGIN software package.

2.4. UV–Vis and FT-IR difference spectroscopy

The recovery kinetics of the ground state of SRI and the fusion constructs with HtrI were monitored at 590 nm using a UV-2401 PC (Shimadzu) spectrophotometer as described previously [10]. A circulating water bath adjusted the measurement temperature to 20 °C. The fusion constructs were illuminated with an orange light emitting diode (Luxeon Star, emission maximum at 589 nm, 21 nm FWHM) with the emission maximum closely matching the absorption maximum of SRI. FT-IR experiments were performed essentially as described [10,15]. Difference spectra were collected at pH 5.5 and 20 °C using a temperature-controlled ATR-IR cell mounted in the sample chamber of the FT-IR spectrometer (IFS 66v/S, Bruker Optics, Ettlingen, Germany). The samples were illuminated with the same orange LED as above. A broadband interference filter limited the spectral range from 1900 to 850 cm^{-1}.

3. Results

According to the sequence alignments and secondary structure predictions [16], there are four tyrosine residues on helix G of SRI, namely Y197, Y208, Y210 and Y213, which may be potentially involved in the hydrogen-bonding interactions with the transducer (Fig. 1). We tested the relevance of these Tyr residues for the receptor-transducer interaction by exchanging them for phenylalanines (denoted SRI_{YxF}). The SRI mutants were fused to a N-terminal 147 residue variant of HtrI (denoted as SRI_{YxF}–$HtrI_{1-147}$). This construct is suitable to the interaction of wild-type SRI and HtrI as judged by the ability to close the proton-conducting channel of SRI which rendered the photocycle kinetics pH-independent [17,18]. The interactions of SRI and the SRI_{YxF} mutants with the transducer $HtrI_{1-147}$ were characterized by isothermal titration calorimetry and time-resolved visible spectroscopy prior to the molecular analysis provided by FT-IR difference spectroscopy.

3.1. Isothermal titration calorimetry

The binding affinities of the transducer to the SRI_{YxF} mutants were determined by using isothermal titration calorimetry. Here, $HtrI_{1-147}$ was titrated with wild-type SRI or the tyrosine mutants of SRI, respectively. Table 1 summarizes the resulting dissociation constants (K_d = 1.4–2.2 μM). They closely agree with the K_d of wild-type SRI–$HtrI_{1-147}$ (K_d = 1.5 μM) demonstrating that the Tyr to Phe mutations did not affect the receptor-transducer binding properties. The comparison to the K_d of wild-type SRI titrated with the truncated transducer $HtrI_{1-52}$ (the N-terminal 52 residues of HtrI, [10]) which exhibited an impaired receptor-transducer interaction (K_d = 9.2 μM), reinforces this conclusion. Another interesting observation emerges from the comparison to the SRII–HtrII complex for which the K_d is one order of magnitude lower (K_d ~ 0.2 μM) [14]. This comparison supports the notion that the binding interaction of HtrI to SRI is weaker than that found in the SRII–HtrII complex.

3.2. Influence of the tyrosine mutations on the recovery kinetics of the SRI–HtrI complex

All spectroscopic experiments were conducted with the fusion constructs (SRI–$HtrI_{1-147}$) to ensure full occupancy of receptor with transducer. Continuous orange–light illumination converts SRI into the long-lived S_{373} photointermediate. We monitored the recovery of ground-state SRI from the photostationary state by recording the kinetics at 590 nm. Fig. 2 depicts the recovery kinetics of the SRI_{YxF}–$HtrI_{1-147}$ fusion proteins at pH 5.5 (black lines) and 7.5 (blue lines). Kinetics of the wild-type phenotype is also included for comparison (red line). The kinetic traces were not significantly affected by the external pH, arguing for an unimpaired functionality of the SRI_{YxF}–$HtrI_{1-147}$ fusion proteins [10,18]. Close inspection of the time traces of SRI_{Y210F}–$HtrI_{1-147}$ reveals, however, that the recovery of the ground state is slightly retarded by about a factor of two, indicating that Y210 of SRI is involved in the interaction with HtrI.

3.3. FT-IR difference spectroscopy of the SRI_{YxF}–$HtrI_{1-147}$ fusion constructs

Light-induced FT-IR difference spectroscopy was applied to examine the structural changes occurring upon transition to the S_{373} photointermediate in the complex. This method is well-suited to probe minute absorbance changes because the difference spectrum exhibits bands characteristic only for the molecular groups that are modified during protein activity [19–22]. Fig. 3 depicts the difference spectra of

Table 1
Dissociation constants (K_d) of wild-type SRI and the tyrosine mutants of SRI in complex with $HtrI_{1-147}$ at + 20 °C. The K_d of wild-type SRI with the shortened transducer $HtrI_{1-52}$ is given for comparison but at + 25 °C. The elevated temperature in the latter ITC experiments did only slightly affect the K_d as demonstrated by the comparison of the K_d of SRI + $HtrI_{1-147}$ at 20 °C and 25 °C (see first row).

Protein complex	K_d (μM)	
	20 °C	25 °C
SRI + $HtrI_{1-147}$	1.5	1.15
SRI_{Y197F} + $HtrI_{1-147}$	2.2	
SRI_{Y208F} + $HtrI_{1-147}$	2.0	
SRI_{Y210F} + $HtrI_{1-147}$	2.2	
SRI_{Y213F} + $HtrI_{1-147}$	1.4	
SRI + $HtrI_{1-52}$		9.2

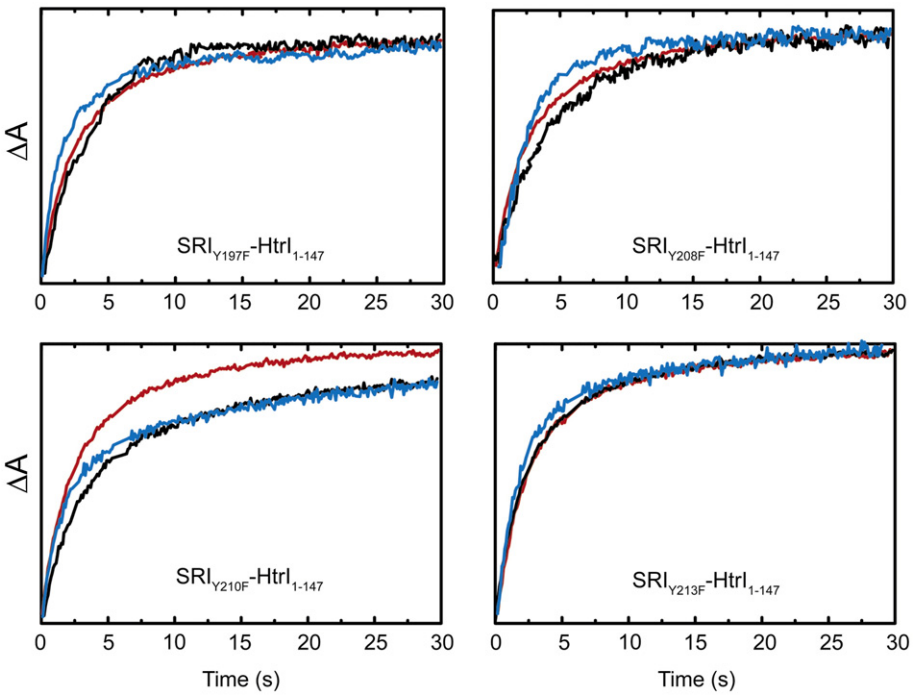

Fig. 2. Comparison of the light-induced absorbance changes monitored at 590 nm of SRI$_{YxF}$–HtrI$_{1-147}$ fusion complexes for pH 5.5 (black) and pH 7.5 (blue) to that of the wild-type SRI–HtrI fusion complex (pH 5.5, red). The traces were normalized to the same initial absorbance to facilitate comparison.

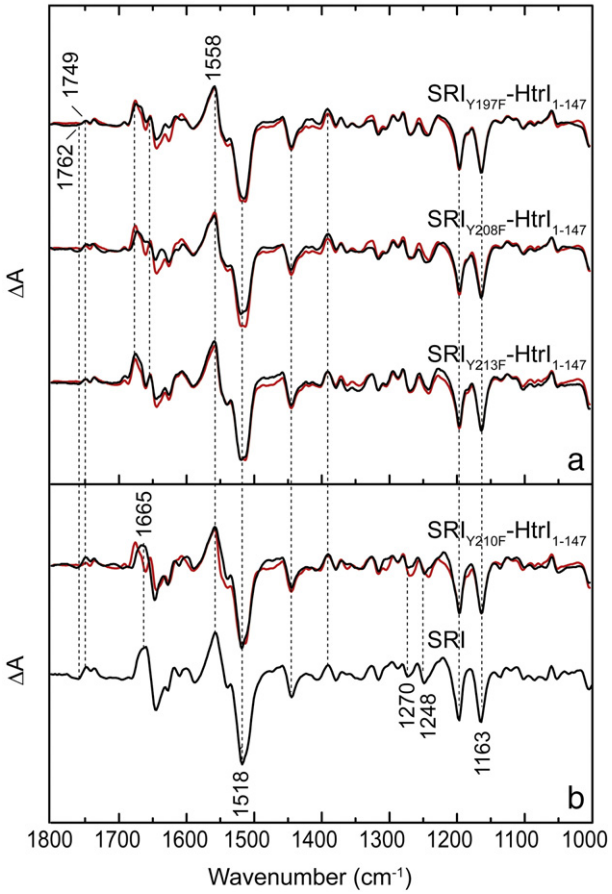

Fig. 3. FT-IR difference spectra (light minus dark) of the SRI$_{Y197F}$–HtrI$_{1-147}$, SRI$_{Y208F}$–HtrI$_{1-147}$, SRI$_{Y213F}$–HtrI$_{1-147}$ (panel a) and of SRI$_{Y210F}$–HtrI$_{1-147}$ and wild-type SRI (panel b) recorded under photostationary conditions. The SRI$_{YxF}$–HtrI$_{1-147}$ spectra (black lines) were compared to that of wild-type SRI–HtrI$_{1-147}$ (red lines). Spectra were normalized on the same intensity of the retinal band at 1163 cm^{-1}.

the SRI$_{YxF}$–HtrI$_{1-147}$ fusion complexes as compared to that of the wild-type complex. Here, the positive bands are characteristic for the S_{373} whereas the negative bands reflect the resting state [10,23,24].

Overall, the spectra are very similar demonstrating that S_{373} is the only photoproduct accumulated under photostationary conditions in all protein constructs used in the study. The intense negative band at 1518 cm^{-1} is assigned to the C=C symmetric stretch mode of the ground-state retinal. The corresponding mode of the S_{373} state contributes to the broad positive band at 1558 cm^{-1}. In the region characteristic for C=O stretch vibrations of protonated carboxylic residues, the differential band at 1762(−)/1749(+) cm^{-1} appears in all spectra and was assigned to protonated D76 of SRI, the proton acceptor in the purple form of SRI [25].

The C=O stretching vibrations of the peptide linkage of the apoprotein (amide I band in the region 1690–1620 cm^{-1}), are strongly altered in the presence of the transducer. These difference bands are sensitive markers for large structural rearrangements generated by the signal relay from SRI to HtrI [10,24]. It is noted from the detailed inspection that the difference spectrum of the mutant SRI$_{Y210F}$–HtrI$_{1-147}$ exhibited a broad positive band at 1665 cm^{-1} (Fig. 3b, upper black curve) which was present neither in the other SRI$_{YxF}$–HtrI$_{1-147}$ fusion proteins nor in the wild-type complex. However, a similar band appeared in the spectrum of SRI in the absence of transducer as well (Fig. 3b, bottom curve). These structural changes also affect the amide II vibrations (out-of-phase coupling of the N–H bend and C–N stretch vibrations, 1580–1520 cm^{-1}) where the broad positive band at 1558 cm^{-1} altered its profile in the SRI and SRI$_{Y210F}$–HtrI$_{1-147}$ spectra (Fig. 4). The small deviations in the spectral domain between 1400 to 1220 cm^{-1} (Fig. 3b, upper curve) are due to changes of the amide III vibration (in-phase coupling of the N–H bend and C–N stretch vibrations) that tally with those of amide I and II vibrations. These observations together with the overall similarity of the SRI$_{Y210F}$–HtrI$_{1-147}$ and SRI spectra further argue that the mutation of Y210 to F impairs the functional interaction between the receptor and transducer in the SRI$_{Y210F}$–HtrI$_{1-147}$ fusion complex. Thus, the IR spectroscopic analysis strongly suggests Y210 as a key residue for the signal transmission from SRI to HtrI.

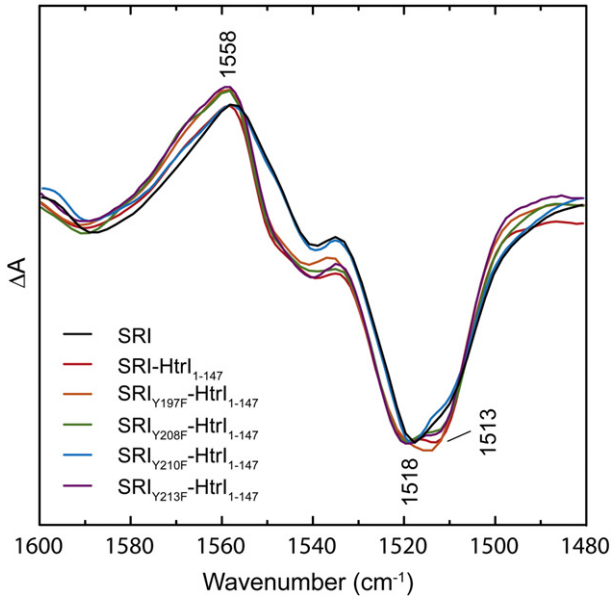

Fig. 4. Zoom-out of the wild-type SRI and SRI–HtrI$_{1-147}$, and SRI$_{YxF}$–HtrI$_{1-147}$ spectra in the 1600–1480 cm^{-1} spectral domain. The negative peak at 1513 cm^{-1} is attributed to the phenyl ring vibration of Y210 (see text).

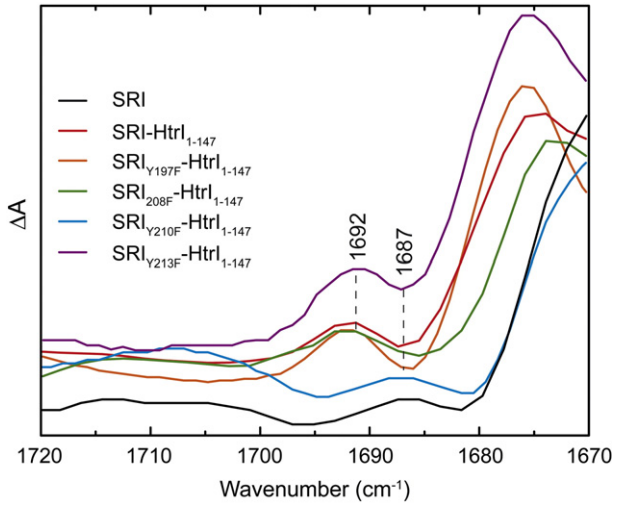

Fig. 5. Zoom-out of the wild-type SRI and SRI–HtrI$_{1-147}$, and SRI$_{YxF}$–HtrI$_{1-147}$ spectra in the 1720–1670 cm^{-1} spectral domain. The differential band at 1692(+)/1686(−) cm^{-1} was assigned to the C=O stretching vibration of the side chain of N53 (see text and [10]).

To evaluate the role of Y210 on the molecular level, we analyzed the difference spectra in the frequency range of the tyrosine vibrations. The phenolic ring mode ($\nu_{(C\,C)}$, $\delta_{(C-H)}$) absorbes at around 1517 cm^{-1} and the $\delta_{(C-O-H)}$ mode at 1169–1260 cm^{-1} [26]. Although these two frequency ranges are congested by retinal and amide modes of the SRI–HtrI complex, contributions from tyrosine modes could be clearly identified. The large negative feature at 1518 cm^{-1} which is due to the C=C stretch of retinal, has a clear shoulder at 1513 cm^{-1} that is completely absent in the spectra of SRI and SRI$_{Y210F}$–HtrI$_{1-147}$ (Fig. 4). In the lower frequency range, the small negative bands at 1270 and 1248 cm^{-1} lack some components only in the SRI and SRI$_{Y210F}$–HtrI$_{1-147}$ difference spectra (Fig. 3b). The former band was also found in the SRII–HtrII difference spectra and it was assigned to the protonated Y199 in SRII [27]. Consequently, we assign the observed bands to the phenolic modes of Y210 which undergoes hydrogen bonding changes upon formation of the signalling state in the SRI–HtrI complex.

In our previous work [10], we reported that a differential band of the SRI–HtrI$_{1-147}$ spectrum at 1692(+)/1686(−) cm^{-1} is attributable to hydrogen bonding changes of N53 of HtrI. Therefore, it was interesting to see if the spectral features of N53 are affected by the Y210F mutation (Fig. 5). Indeed, careful examination of the spectral domain characteristic for C=O stretching modes of Asn side chains (1700–1680 cm^{-1}) reveals that the differential band at 1692(+)/1686(−) cm^{-1} is missing in the spectra of SRI and SRI$_{Y210F}$–HtrI$_{1-147}$ but is present in those of all other proteins. From these results it is evident that the observed bands of N53 and Y210 are interdependent.

In conclusion, the present IR experiments demonstrated that Y210 of SRI is the hydrogen bonding donor to the carbonyl oxygen of N53 of HtrI when they form the complex, which bears great relevance for the mechanism of the signal relay.

4. Discussion

Our search for the molecular basis of the receptor–transducer communication in the SRI–HtrI signaling complex was based on the comparison to the SRII–HtrII complex from *N. pharaonis*. There, the crystal structure revealed a hydrogen bond between helix G (Y199) and TM2 (N74), roughly in the middle of the membrane [3]. In an earlier study, we demonstrated that N53 of HtrI is involved in a hydrogen bond that is essential for the signal transfer in the SRI–HtrI complex [10]. However, the hydrogen-bonding partner was unknown. Guided by the hydrogen-bonding interaction in the SRII–HtrII complex, we substituted the four tyrosine residues on helix G of SRI (Fig. 1) by phenylalanine to investigate their roles in the binding and functional properties in the receptor–transducer complex.

ITC experiments showed that the ability of SRI to associate with HtrI was not affected by any of the mutations as the dissociation constants of the mutated complexes did not differ significantly from the wild type. Noteworthy, the dissociation constant of the SRI–HtrI complex (Table 1) is one order of magnitude weaker than that found for the SRII–HtrII complex [14] which might be of functional relevance.

Consistent with the calorimetric data, the Tyr mutations do not alter the photochemical characteristics of SRI in the complex (Fig. 2) except for the Y210F mutant which exhibits slightly slower kinetics. This observation spots Y210 as a relevant residue for the complex functionality. Interestingly, substitutions of the transducer N53 residue by Ala, Asp or Gln critically retarded the recovery kinetics of the ground-state by a factor of 10 [10]. This mismatch may argue against the direct coupling between Y210 and N53 in the structural model of the SRI–HtrI complex (Fig. 1). Several publications proposed that the photoactive center of SRI and the cytoplasmic end of TM2 are interconnected via a network of ionic and hydrogen bonds and this interconnection is responsible for the inhibition of proton pumping in SRI [18,28,29]. Our previous findings [10] supported this suggestion as they indicated that the structural changes of protonated D76 are influenced by N53 mutation. Thus, N53 seems to be an important component of this hydrogen-bonded network and, therefore, its removal would affect other receptor-transducer contacts than solely the Y210–N53 hydrogen bond.

Conclusive information about the influence of the tyrosine mutations on the complex functionality is provided by the FT-IR difference spectra (Fig. 3). Here, the vibrational bands characteristic for protein structural changes are critically distorted upon receptor complexation. The spectrum of the Y210 mutant in the SRI–HtrI complex is very similar to the difference spectra of the receptor SRI only, whereas the spectra of the other Tyr mutants are identical to those of the wild-type complex. The similar features in the spectra of SRI and SRI$_{Y210F}$–HtrI$_{1-147}$ mutant (Fig. 3b) argue for a loss of complex function induced by the Y210F mutation. Several bands that are lacking in the spectrum of SRI$_{Y210F}$–HtrI$_{1-147}$ but are present in the other spectra, were identified to originate from Y210 structural

alterations that are generated by HtrI activation (Fig. 4). The most definitive evidence in favor of a communication between Y210 and N53 is the dissapearance of the N53 bands upon Y210F mutation (Fig. 5). From these results, we conclude that Y210 and N53 form a hydrogen bond which is significant for the inter-protein signal transmission in the SRI–HtrI complex. This finding agrees well to the SRII–HtrII complex where the crystallographic structure identified the direct mutual interaction between Y199 and N74 via an inter-helical hydrogen bond [3]. Interestingly, the formation of the signaling states causes opposite changes in hydrogen bonding in these two complexes as it is weaker in SRI–HtrI but stronger in SRII–HtrII [27,30]. It is debatable whether the observed hydrogen bond changes correlate with the repellent and/or attractant responses in phototaxis that is mediated by the respective SR–Htr complexes. Thus, it will be worthwhile to find out how the hydrogen bond of Y210 and N53 changes in the repellent forms of SRI–HtrI [31,32]. Such experiments are currently underway.

Acknowledgments

This work was supported by grants from the Deutsche Forschungsgemeinschaft (SFB 613, K8) to J.H. We thank Ina Ehring (Bielefeld), Ilona Ritter and Ramona Justinger (Jülich) for excellent technical assistance.

Appendix A. Supplementary data

Supplementary data associated with this article can be found, in the online version, at doi:10.1016/j.bpc.2010.02.017.

References

[1] W.D. Hoff, K.H. Jung, J.L. Spudich, Molecular mechanism of photosignaling by archaeal sensory rhodopsins, Annu. Rev. Biophys. Biomol. Struct. 26 (1997) 223–258.
[2] X. Chen, J.L. Spudich, Demonstration of 2:2 stoichiometry in the functional SRI–HtrI signaling complex in Halobacterium membranes by gene fusion analysis, Biochemistry 41 (2002) 3891–3896.
[3] V.I. Gordeliy, J. Labahn, R. Moukhametzianov, R. Efremov, J. Granzin, R. Schlesinger, G. Büldt, T. Savopol, A.J. Scheidig, J.P. Klare, M. Engelhard, Molecular basis of transmembrane signalling by sensory rhodopsin II-transducer complex, Nature 419 (2002) 484–487.
[4] A.A. Wegener, J.P. Klare, M. Engelhard, H.J. Steinhoff, Structural insights into the early steps of receptor–transducer signal transfer in archaeal phototaxis, EMBO J. 20 (2001) 5312–5319.
[5] D.D. Oprian, Phototaxis, chemotaxis and the missing link, Trends Biochem. Sci. 28 (2003) 167–169.
[6] X.N. Zhang, J.Y. Zhu, J.L. Spudich, The specificity of interaction of archaeal transducers with their cognate sensory rhodopsins is determined by their transmembrane helices, Proc. Natl. Acad. Sci. USA 96 (1999) 857–862.
[7] R.A. Bogomolni, J.L. Spudich, The photochemical reactions of bacterial sensory rhodopsin-I. Flash photolysis study in the one microsecond to eight second time window, Biophys. J. 52 (1987) 1071–1075.
[8] E.N. Spudich, J.L. Spudich, The photochemical reactions of sensory rhodopsin I are altered by its transducer, J. Biol. Chem. 268 (1993) 16095–16097.
[9] R. Moukhametzianov, J.P. Klare, R. Efremov, C. Baeken, A. Goppner, J. Labahn, M. Engelhard, G. Buldt, V.I. Gordeliy, Development of the signal in sensory rhodopsin and its transfer to the cognate transducer, Nature 440 (2006) 115–119.
[10] O.S. Mironova, I.L. Budyak, G. Büldt, R. Schlesinger, J. Heberle, FT-IR difference spectroscopy elucidates crucial interactions of sensory rhodopsin I with the cognate transducer HtrI, Biochemistry 46 (2007) 9399–9405.
[11] G. Schmies, I. Chizhov, M. Engelhard, Functional expression of His-tagged sensory rhodopsin I in *Escherichia coli*, FEBS Lett. 466 (2000) 67–69.
[12] M.P. Krebs, E.N. Spudich, J.L. Spudich, Rapid high-yield purification and liposome reconstitution of polyhistidine-tagged sensory rhodopsin I, Protein Expr. Purif. 6 (1995) 780–788.
[13] O.S. Mironova, R.G. Efremov, B. Person, J. Heberle, I.L. Budyak, G. Büldt, R. Schlesinger, Functional characterization of sensory rhodopsin II from *Halobacterium salinarum* expressed in *Escherichia coli*, FEBS Lett. 579 (2005) 3147–3151.
[14] S. Hippler-Mreyen, J.P. Klare, A.A. Wegener, R. Seidel, C. Herrmann, G. Schmies, G. Nagel, E. Bamberg, M. Engelhard, Probing the sensory rhodopsin II binding domain of its cognate transducer by calorimetry and electrophysiology, J. Mol. Biol. 330 (2003) 1203–1213.
[15] I. Radu, C. Bamann, M. Nack, G. Nagel, E. Bamberg, J. Heberle, Conformational changes of channelrhodopsin-2, J. Am. Chem. Soc. 131 (2009) 7313–7319.
[16] A. Blanck, D. Oesterhelt, E. Ferrando, E.S. Schegk, F. Lottspeich, Primary structure of sensory rhodopsin I, a prokaryotic photoreceptor, EMBO J. 8 (1989) 3963–3971.
[17] B. Perazzona, E.N. Spudich, J.L. Spudich, Deletion mapping of the sites on the HtrI transducer for sensory rhodopsin I interaction, J. Bacteriol. 178 (1996) 6475–6478.
[18] X. Chen, J.L. Spudich, Five residues in the HtrI transducer membrane-proximal domain close the cytoplasmic proton-conducting channel of sensory rhodopsin I, J. Biol. Chem. 279 (2004) 42964–42969.
[19] R. Vogel, F. Siebert, Vibrational spectroscopy as a tool for probing protein function, Curr. Opin. Chem. Biol. 4 (2000) 518–523.
[20] C. Kötting, K. Gerwert, Proteins in action monitored by time-resolved FTIR spectroscopy, Chem.Phys. Chem. 6 (2005) 881–888.
[21] R.M. Nyquist, K. Ataka, J. Heberle, The molecular mechanism of membrane proteins probed by evanescent infrared waves, Chem. Biochem. 5 (2004) 431–436.
[22] I. Radu, M. Schleeger, C. Bolwien, J. Heberle, Time-resolved FT-IR difference spectroscopy and the application to membrane proteins, Photochem. Photobiol. Sci. 8 (2009) 1517–1528.
[23] O. Bousche, E.N. Spudich, J.L. Spudich, K.J. Rothschild, Conformational changes in sensory rhodopsin I: similarities and differences with bacteriorhodopsin, halorhodopsin, and rhodopsin, Biochemistry 30 (1991) 5395–5400.
[24] Y. Furutani, H. Takahashi, J. Sasaki, Y. Sudo, J.L. Spudich, H. Kandori, Structural changes of sensory rhodopsin I and its transducer protein are dependent on the protonated state of Asp76, Biochemistry 47 (2008) 2875–2883.
[25] P. Rath, E. Spudich, D.D. Neal, J.L. Spudich, K.J. Rothschild, Asp76 is the Schiff base counterion and proton acceptor in the proton- translocating form of sensory rhodopsin I, Biochemistry 35 (1996) 6690–6696.
[26] A. Barth, C. Zscherp, What vibrations tell us about proteins, Q. Rev. Biophys. 35 (2002) 369–430.
[27] V.B. Bergo, E.N. Spudich, K.J. Rothschild, J.L. Spudich, Photoactivation perturbs the membrane-embedded contacts between sensory rhodopsin II and its transducer, J. Biol. Chem. 280 (2005) 28365–28369.
[28] R.A. Bogomolni, W. Stoeckenius, I. Szundi, E. Perozo, K.D. Olson, J.L. Spudich, Removal of transducer HtrI allows electrogenic proton translocation by sensory rhodopsin I, Proc. Natl. Acad. Sci. USA. 91 (1994) 10188–10192.
[29] K.H. Jung, J.L. Spudich, Protonatable residues at the cytoplasmic end of transmembrane helix-2 in the signal transducer HtrI control photochemistry and function of sensory rhodopsin I, Proc. Natl. Acad. Sci. USA. 93 (1996) 6557–6561.
[30] Y. Furutani, K. Kamada, Y. Sudo, K. Shimono, N. Kamo, H. Kandori, Structural changes of the complex between pharaonis phoborhodopsin and its cognate transducer upon formation of the m photointermediate, Biochemistry 44 (2005) 2909–2915.
[31] J. Sasaki, B.J. Phillips, X. Chen, E.N. Van, A.L. Tsai, W.L. Hubbell, J.L. Spudich, Different dark conformations function in color-sensitive photosignaling by the sensory rhodopsin I-HtrI complex, Biophys. J. 92 (2007) 4045–4053.
[32] O.A. Sineshchekov, J. Sasaki, B.J. Phillips, J.L. Spudich, A Schiff base connectivity switch in sensory rhodopsin signaling, Proc. Natl. Acad. Sci. U.S.A. 105 (2008) 16159–16164.